Generic resonator models for real-time synthesis of reed and brass instruments

Ph Guillemain, Jean Kergomard

Forum Acusticum 2011 - Aalborg - Denmark

Generic resonator models for real-time synthesis of reed and brass instruments

Ph. Guillemain*, J. Kergomard
Laboratoire de Mécanique et d'Acoustique, CNRS UPR 7051
31 Chemin Joseph Aiguier, 13402 Marseille Cedex 20, France. *Currently at: Laboratoire d'Acoustique de l'Université du Maine, Avenue Olivier Messiaen, 72085 Le Mans Cedex 9

Summary
From accurate measurements of bore profiles of various reed and brass instruments, a common and simplified geometrical model made of three parts totalizing seven geometrical parameters is proposed. From this geometry, it is shown that a good approximation of the input impedance can be obtained by a combination of two lumped elements gathered in series and parallel with a distributed element. Each element is approximated and discretized in order to end up with costless digital filters representing the impedance impulse response. These filters require the order of twenty multiplication/additions per sample and their coefficients are analytically expressed as functions of the geometrical parameters. The choice of the geometry and the time discretization schemes are validated both through comparison with continuous models and through the estimation of the geometrical parameters via a global optimization procedure, using measured input impedance curves.

PACS no. 43.75.Ef, 43.75.Pq

1. Introduction

This paper aims at providing simple, yet accurate, digital models of the input impedances of conical woodwinds and brass instruments, for use in the context of real-time sound synthesis.

Many studies have been devoted to the modeling of acoustic bores. In the context of the direct problem, consisting in calculating the input impedance from a measured geometry, Caussé et al. [5], have shown a very good accordance between models and measurements in the case of brasses. In the context of the inverse problem, consisting in reconstructing a bore profile [1, 18] from measurement, many methods have been developped, some of them leading to commercial devices citekausel.

The underlying physical model of the instrument bore calls the use of transfer matrices representing the geometrical assembly constituting the instrument. Unfortunately, for many elements citebenade1,scavone1,kergomard1, the conversion of the models [20] or the measurements [8] in terms of stable and costless digital filters usable for real-time sound synthesis is not straightforward. Most attempts, based on the wave variables representations [19, 21] have been devoted to the accurate digital modeling of specific elements and their assembly rather than on simplified models of the whole bore.

The scope of this paper is to focus on the *synthesis* rather than on the *simulation* point of view. Some specific requirements of the synthesis approach can be summarized as follows: The resonator of the instrument is just one part of the whole functioning model which also includes flow models and excitor-dynamics models (see *e.g.* [17]). In this context, the success of a synthesis process is mostly based on a subjective judgement involving both playability and timbre naturalness. Finally, from a digital instrument design point of view, the simplicity of the model and its small number of degrees of freedom are important features which prevent the loss of generality and facilitates its handling and timbre extrapolation.

This paper investigates both the direct and inverse problems by providing digital impedance models fully defined from coarse and flexible geometries and by validating the use of these geometries and the discretization schemes from the analysis and synthesis of measured impedances.

The paper is organized as follows: Section 2 briefly presents the fine geometries of three saxophones and one trumpet and how they can be gathered into more global elements. In section 3, simplified digital models for conical bores and Bessel horns are presented and an assembly of the main bore and the mouthpiece, common to saxophones and brasses is proposed. Sec-

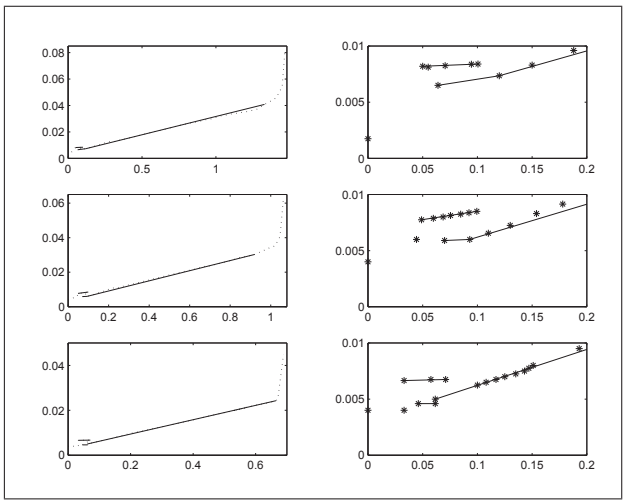

Figure 1. From top to bottom: bore profiles of a tenor, an alto and a soprano saxophone. Vertical axis: radius, in m. Horizontal axis: length, in m. Right panels: blow-up of left panels on the first $0.2m$. The stars correspond to the measured values (after Nederveen).

tion 4 deals with the estimation of the model parameters from measured impedance curves.

2. Simplified geometrical models

In this section, from geometrical measurements made by Nederveen [13] and Caussé, a simplified geometrical model of saxophone-like and brass-like instruments is presented.

2.1. Saxophone model

The left panels of figure 1 show in dotted lines, from top to bottom, the measured radii of tenor, alto, and soprano saxophone. The right panels show a blow up on the first $0.2m$ of each bore. For both panels, straight solid lines correspond to a hand-made sectionning of the whole bore into three parts. The first part represents the mouthpiece and will be considered as an acoustic compliance. The second part, called the backbore along this paper, represents the part of the main bore surrounded by a cork on which the mouthpiece is plugged. It is a cone of small length, with a top angle smaller than that of the main bore. The third and main part of the bore is made of a long conical bore. The short bell ending the conical bore will be ignored, as well as the tonehole network.

2.2. Trumpet model

The left panel of figure 2 shows in dotted lines, the measured radii of a trumpet with respect to the distance from the bore input. The right panel shows a blow up of the measured values on the first $0.2m$. The main bore is assumed to be a cylinder prolongated by a Bessel horn. The mouthpiece is made of a short divergent bore, the input radius of which is much smaller than that of the cylinder, and a convergent bore whose input radius is much larger than that of the cylinder (see *e. g.* [15]).

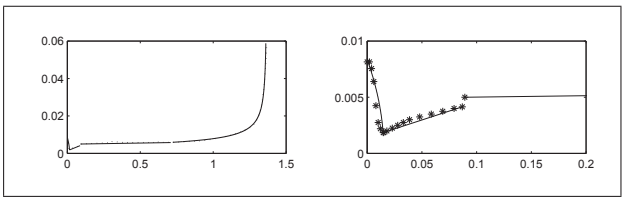

Figure 2. Bore profile of a trumpet. Vertical axis: radius, in m. Horizontal axis: length, in m. Right panel: blow-up of left panel on the first $0.2m$. The stars correspond to the measured values (after Caussé).

3. Digital impedance models

3.1. Main bore models

Continuous input impedance models and their digital versions are presented in the case of conical bores and Bessel horns.

3.1.1. Saxophone bore

Continuous model: The main bore is assumed to be conical with input radius R_2, top angle θ_2 and whose effective length L_2 corresponds to that of the first open tonehole. Its input impedance denoted Z_2 is classically written:

$$Z_2 = Z_{c_2} \frac{1}{\frac{1}{j\tan(kL_2)} + \frac{1}{jkx_e}} \tag{1}$$

where $x_e = R_2/\sin(\theta_2/2)$ is the length of the missing part of the cone and $Z_{c_2} = \rho c/(\pi R_2^2)$ is the characteristic impedance. The wavenumber $k = k(\omega)$ includes viscothermal losses [14].

For various lengths, top angles and input radii, using stepped cone models made of an association of one thousand small cylinders, it has been determined that the radius R used to compute the losses could be taken as the radius corresponding to the average losses while the losses in the term $1/(jkx_e)$ could be ignored: $\frac{L_2}{R} = \int_{x_e}^{L_2+x_e} \frac{dx}{R(x)}$ which gives, since $R(x) = R_2 x/x_e$:

$$R = \frac{R_2}{\mu_2} \frac{L_2}{x_e \ln\left(1 + \frac{L_2}{x_e}\right)} \tag{2}$$

where the control parameter μ_2 is used as an additional mean to adjust the losses.

Discrete model: The digital model of the main conical bore is built according to [9]. The losses are modelled with a first order low-pass filter. If F_e is the sampling rate and $z = \exp(j\omega/F_e)$, $\exp(-2jkL_2)$ is approximated by the filter: $\frac{b_0}{1-a_1 z^{-1}} z^{-D}$ and the element jkx_e is discretized with the bilinear transformation: $jkx_e \simeq 2F_e(1-z^{-1})/(1+z^{-1})x_e/c$.

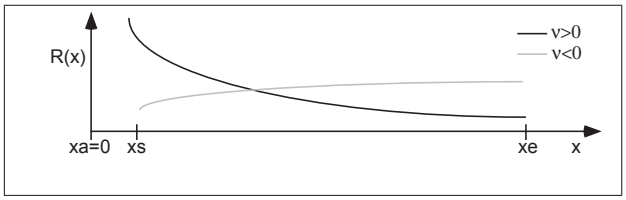

Figure 3. Geometry of the Bessel horn.

3.1.2. Brass bore

It is assumed that the radius of the horn part of the bore is modelled by: $R(x) = R_2 x_e^\nu / x^\nu$ and that this bore is prolongated by a cylindrical bore of length l_c. The discussion is limited to the case $\nu \in [-1, 1]$. As depicted in figure 3, x_e and x_s denote the coordinates of the input and the output, respectively, and $x_a = 0$ is the asymptote. The input radius $R(x_e)$ is denoted R_2.

Continuous model: In the divergent case ($\nu > 0$), it is assumed that x_s is close to the asymptote $x_a = 0$. If kx_e is large, by ignoring the radiation impedance and denoting $Z_c = \rho c/(\pi R_2^2)$ the characteristic impedance, the input impedance can be written as [6]:

$$Z_e = jZ_c \tan\left(k(x_e + l_c) - \nu\frac{\pi}{2}\right) \tag{3}$$

This shows that for positive frequencies, the input impedance is a translated version of $-\nu c/(4l_e)$ of the input impedance of a cylindrical bore with length $l_e = l_c + x_e$.

As it has been done for the cone case, frequency-dependent losses are taken into account through a modification of the input radius of the horn part of the bore, yielding:

$$R = \frac{x_e - x_s}{\int_{x_e}^{x_s} \frac{dx}{R(x)}} = \frac{R_2}{\mu_2}(1 + \nu) \tag{4}$$

Discrete model for $\nu < 0$: It is worth noting that Z_e is the impedance of a cylindrical bore element with length l_e terminated at x_s in an element with a purely imaginary impedance: $Z_t = jZ_c \tan(-\nu\pi/2)$. Since for positive values of ν, Z_t is negative and the impulse response associated to Z_e contains increasing exponentials [20], only the case $\nu < 0$ can insure a passive discrete system and this is why the discrete time model is built first from the case $\nu < 0$.

For digital efficiency, it is proposed to terminate a cylinder of length L in a lumped element, the impedance of which is a derivator and the associated reflection coefficient is an all-pass filter. At low frequency, this termination acts as a length increase, the effect of which is to decrease the frequencies of the first peaks, therefore corresponding to the case $\nu < 0$.

Let C and P denote the dimensionless impedances of the cylinder and the termination, respectively:

$$C = \frac{1 - \exp(-2jkL)}{1 + \exp(-2jkL)}, \quad P = r_p j\omega \tag{5}$$

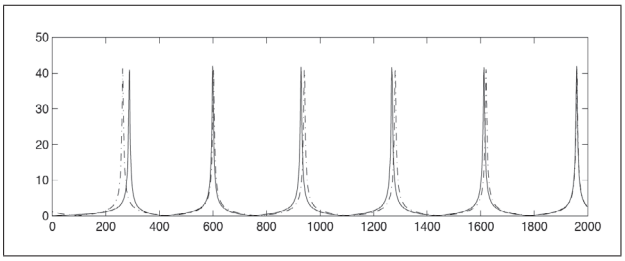

Figure 4. Modulus of Z_e in dashed-dotted line and of $\tilde{Z}_b$ in solid line. Bore parameters: $\nu = 0.55$, $x_e = 0.5m$, $x_s = 0.01m$, $R_2 = 7mm$.

The total impedance is:

$$\tilde{Z}_e = Z_c \frac{P + C}{1 + PC} \tag{6}$$

In order to approximate Z_e with $\tilde{Z}_e$, analytic expressions of r_p and L as functions of ν and l_e can be obtained using the approximation: $\arctan(x) \simeq \frac{\pi}{2}\frac{x}{1+x}$ assuming frequency independant losses. The values of the parameters are determined so that the frequency of two selected peaks are the same for the continuous and the digital models.

Discrete model for $\nu > 0$: The digital impedance model corresponding to the case $\nu > 0$ is built by noticing that the impedance of a Bessel horn with $\nu = 1$ is the admittance of a cylinder (or the impedance of a closed cylinder, hence exhibiting a peak at zero frequency) to which is substracted a low frequency approximation of this peak. Indeed, the input impedance is exactly given by:

$$Z_e = \frac{1}{j\tan(kl_e)} - \frac{1}{jkl_e} \tag{7}$$

This suggests to start from the admittance associated to the impedance model proposed for $\nu < 0$ (equation (6)) as the dimensionless impedance for $\nu > 0$ and to remove its zero frequency peak.

The peak at zero frequency is removed using a first order Taylor expansion of $\tilde{Z}_e$ at $\omega = 0$ yielding a total impedance, denoted $\tilde{Z}_b$ as:

$$\tilde{Z}_b = \frac{1}{\tilde{Z}_e} - \frac{1}{d_0 + d_1\mathcal{D}} \tag{8}$$

where $\mathcal{D}$ is the bilinear transform.

The coefficients d_0 and d_1 are determined analytically by considering the value of the impedance at zero frequency, that has to be real and positive and the derivative of the associated reflection function, that has to be zero in order to ensure continuity. The peak matching process used previously leads again to analytical solutions for r_p and L.

Figure 4 shows, for $\nu = 0.55$, $x_e = 0.5m$, $x_s = 0.01m$, $R_2 = 7mm$ and for frequency independent losses, the modulus of Z_e and $\tilde{Z}_b$. The frequencies used for the matching correspond to those of the second and sixth impedance peaks.

3.2. Backbore and mouthpiece models

The backbore is modelled by a small conical element of length L_1 with input radius R_1 and top angle θ_1. Its input impedance will be denoted Z_1 and is:

$$Z_1 = Z_{c_1} \frac{1}{\frac{1}{j\tan(kL_1)} + \frac{1}{jkx_{ee}}} \quad (9)$$

where $x_{ee} = R_1/\sin(\theta_1/2)$ is the length of the missing cone and $Z_{c_1} = \rho c/(\pi R_1^2)$ is the characteristic impedance. Using a low frequency approximation ($j\tan(kL_1) \simeq jkL_1$) and assuming frequency independent losses finaly leads to:

$$Z_1 = Z_{c_1} \frac{x_{ee}}{L_1 + x_{ee}} (G + j\omega \frac{L_1}{c}(1-G)) = Z_{c_1}\mathcal{C}_1 \quad (10)$$

which shows that the conicity of the bore is carried by the coefficient: $x_{ee}/(L_1 + x_{ee})$.

The mouthpiece is also modelled by a lossless short cylindrical element with length L_0 and radius R_0 with input impedance:

$$Z_0 = Z_{c_0} jkL_0 = Z_{c_0}\mathcal{C}_0 \quad (11)$$

The derivations involved in Z_0 and Z_1 are discretized with the bilinear transform. The losses contained in Z_1 are taken into account by considering the value of G for a given frequency, chosen as the resonance frequency ω_h of the whole mouthpiece, constituting a Helmholtz resonator. As it has been done for the main bores, for the sake of flexibility of the model, an additional control parameter μ_1 is used in order to allow a better matching of real losses in the backbore.

3.3. Full bore model

In what follows, $\mathcal{S}_2$ denotes the dimensionless digital impedance corresponding either to the conical bore or to the Bessel horn (Eqs. (1) and (8)).

Since $Z_{c_1} > Z_{c_2}$, the input impedance of the combination backbore/main bore simplifies as a serial combination of elements. In the same way, the total input impedance of the whole bore simplifies as a parallel combination of elements since $Z_{c_0} << Z_{c_1}$. Hence, the final model using dimensionless variables is:

$$Z_e = \frac{1}{Z_{c_2}} \frac{1}{\frac{1}{Z_{c_2}\mathcal{S}_2 + Z_{c_1}\mathcal{C}_1} + \frac{\mathcal{C}_0}{Z_{c_0}}} \quad (12)$$

Equation (12) shows that the combination mouthpiece/backbore acts as a Helmholtz resonator with a cavity volume V_0 such that $\mathcal{C}_0/Z_{c_0} = j\omega V_0/(\rho c^2)$, terminated in the main bore. As a convention, the cavity of the Helmholtz resonator will be considered to be hemispherical, which allows to parametrize it with a unique radius R_0, yielding: $\frac{\mathcal{C}_0}{Z_{c_0}} = j\omega \frac{2\pi R_0^3}{3\rho c^2}$.

For the saxophone case, up to the element of impedance Z_1, which mainly acts as a length correction at low frequencies, this model is similar to that discussed by Dalmont et al. [7]. It is also a simplified version of that discussed in [3] for the oboe case, where it is shown that the role of the backbore of impedance Z_1 is to improve the inharmonicity correction provided by the volume of impedance Z_0.

For direct use of a synthesis scheme such as that already presented by the same authors in [9], Eq. (12) is converted into a difference equation expressing at each sample n the acoustic pressure $p_e(n)$ as function of $u_e(n)$ and the past values of p_e and u_e. Each filter coefficient is expressed analytically with respect to the geometric parameters. The computation cost of the whole digital impedance model is 21 multiplications/additions per signal sample for the brass model and 17 for the saxophone model.

3.4. Examples

The top panel of figure 5 shows, for the tenor saxophone, the impedances obtained with the continuous and digital models. Geometrical values are obtained with the profile shown in figure 1 and are: $L_2 = 1.2m$, $R_2 = 7.35mm$, $\theta_2 = 3.17$, $L_1 = 56mm$, $R_1 = 6.5mm$, $\theta_1 = 1.74$. The volume V_0 corresponds exactly to the missing part of the main conical bore, yielding $R_b = 19.3mm$. The differences between the continuous and the discrete models are not noticeable for both the amplitudes and the frequencies (for example, the frequency differences for the first and fifth peak are respectively $0.5Hz$ and $2Hz$).

The bottom panel shows the same quantities for the trumpet. Geometrical values are obtained from the profile shown in figure 2 and are: $L_2 = 1.28m$, $R_2 = 5mm$, $\nu = 0.5$, $L_1 = 72mm$, $R_1 = 1.85mm$, $\theta_1 = 3.64$. The volume V_0 is estimated by measuring the cup volume, yielding $R_b = 9.1mm$. In the continuous model, the main bore is splitted into a cylindrical bore ($L = 0.62m$) and a Bessel horn ($L = 0.66m$). The most noticeable difference between the continuous and the discrete models lies in the frequency and the height of the first impedance peak. The frequency difference is caused by the choice of the frequencies leading to the solution for r_p and L, corresponding here to the second and sixth impedance peaks. For other significant peaks, the largest frequency difference is obtained for the fourth peak and is $4Hz$.

4. Optimization of geometrical parameters

The aim of the optimization process is to provide the geometrical parameters involed in Eq. (12) from a measured impedance spectrum. The global optimization method used is an evolution strategy with covariance matrix adaptation (CMA-ES) [10], distributed under GNU Public Licence [22]. The optimization process consists in finding the set of parameters:

- R_2, $L2$, μ_2, θ_2 or ν, characterizing the main bore.

(c) European Acoustics Association, ISBN: 978-84-694-1520-7, ISSN: 221-3767

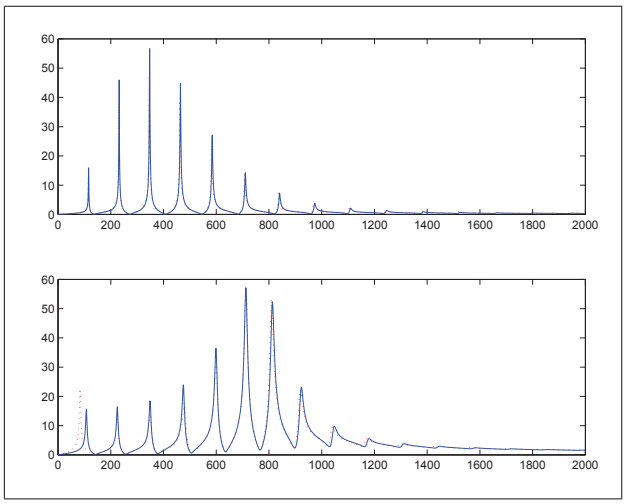

Figure 5. Top panel: Impedance modulus of a tenor saxophone; Bottom panel: Impedance modulus of a trumpet. Dotted line (red): continuous model. Solid line (blue): Digital model.

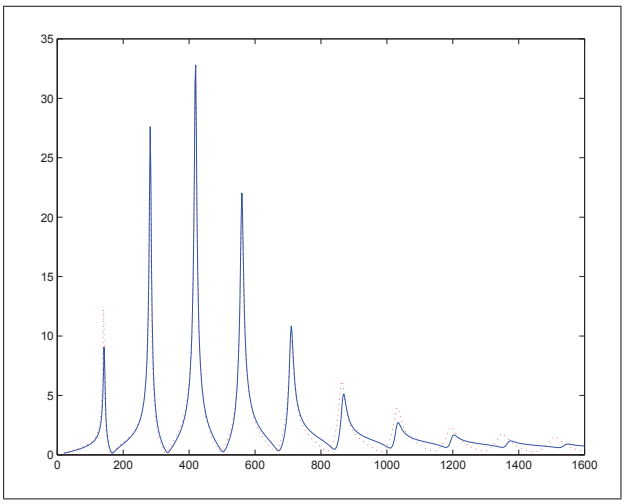

Figure 6. Measured (red dotted lines) alto saxophone impedance and digital model (blue solid line) leading to the minimum of the cost function.

- R_1, L_1, μ_1, R_0, characterizing the backbore and mouthpiece.

According to Eq. (10), the conicity θ_1 of the backbore is taken into account as a modification of Z_{c_1}. In addition to these parameters, since the dimensionless impedance model is normalized with respect to the radius of the main bore, an impedance gain G_z is used to ensure a proper scaling with respect to the measurement. The optimization is constrained: the possible value of each geometrical parameter is bounded. These constraints insure that the global minimum of the cost function leading to geometrically relevant parameters is reached and that the approximations leading to Eq. 12 are satisfied.

The cost function has been chosen as:

$$\Lambda = \left(\int_{\omega_m}^{\omega_M} ||Z_e(\omega)|^p - |Z_{mes}(\omega)|^p| \, d\omega \right)^{1/p} \quad (13)$$

$Z_{mes}(\omega)$ is the measured impedance, p is a real number ($p = 3$ in the examples). Its role is to emphasize the matching of the heights and frequencies of the highest impedance peaks. The frequencies ω_m and ω_M correspond either to the frequency range of the measurements or to a user-defined frequency bandwidth. Working on the modulus of the impedance rather than on the complete impedance allows to get rid of possible phase errors during the measurements.

Figure 6 shows the measured impedance of an alto saxophone and the digital impedance leading to the global minimum of the cost function. The minimisation has been performed on the whole frequency range available in the measure $[20Hz - 1600Hz]$. The estimated geometrical parameters are: $G_z = 1.5$, $L_2 = 0.97m$, $R_2 = 6.61mm$, $\mu_2 = 2.8$, $\theta_2 = 3.5$, $L_1 = 40mm$, $R_1 = 5.52mm$, $\mu_1 = 1$, $R_0 = 17.7mm$. The Helmholtz resonance frequency is $770Hz$ and is close to the "break frequency" related to the cut-off frequency of the tonehole lattice measured in [4] ($837Hz$). The maximum amplitude and frequency errors correspond to the first peak and are $\Delta A/A = 25\%$ and $\Delta f/f = 1.5\%$, respectively. This is natural since the chosen value of p emphasizes the accuracy of the estimation on the higher peaks. For the other peaks whose frequencies are below $1000Hz$, the average $\Delta f/f$ is 0.13% while the average $\Delta A/A$ is 11%.

Figure 7 shows the measured impedance of a trumpet and the impedance yealding the global mininum of the cost function. The minimisation has been performed on the frequency range $[140Hz - 1300Hz]$ and ignores the first impedance peak since it is not used during the play. The estimated geometrical parameters are: $G_z = 3.2$, $L_2 = 1.5m$, $R_2 = 5.8mm$, $\mu_2 = 2.6$, $\nu = 0.76$, $L_1 = 7.1mm$, $R_1 = 1.51mm$, $\mu_1 = 0.4$, $R_0 = 12.8mm$. The Helmholtz resonance frequency is $815Hz$. If the first peak is ignored, the maximum amplitude and frequency errors correspond to the second peak and are respectively $\Delta A/A = 25\%$ and $\Delta f/f = 0.9\%$. For the other peaks whose frequencies are below $1000Hz$, the average $\Delta f/f$ is 0.2% while the average $\Delta A/A$ is 5%. This last value is smaller than in the saxophone case since all the peaks roughly have the same heights.

It can be noticed that, though the frequency and heights of the impedance peaks have been favored in the estimations, the values of the frequencies and amplitudes of the admittance peaks are also accurately reproduced below $1000Hz$ for both the trumpet and the saxophone. It has been checked that the difference above $1000Hz$ is due to the approximation of the backbore and the mouthpiece with lumped elements.

(c) European Acoustics Association, ISBN: 978-84-694-1520-7, ISSN: 221-3767

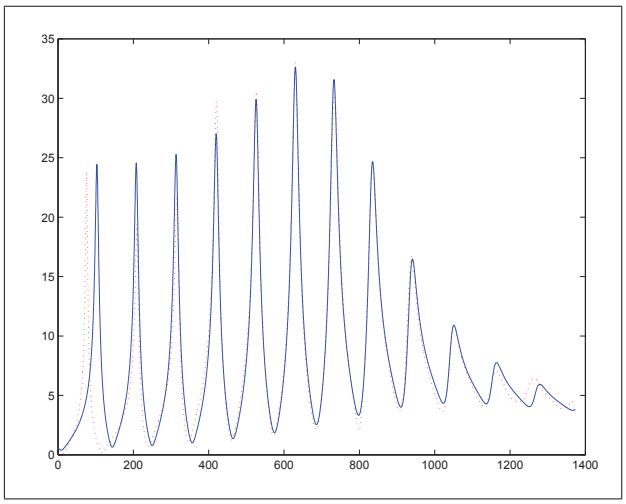

Figure 7. Measured (red dotted lines) trumpet impedance and digital model (blue solid line) leading to the minimum of the cost function.

5. Conclusion

Flexible and numerically efficient digital impedance models can be found using the decomposition of bores of common instruments into three sections. Comparisons with continuous models show a very good accordance, even though drastic approximations to reduce the computation cost are made. The parameters of the digital models obtained from impedance measurements lead to a plausible intrument geometry and this validates the approximations made from the synthesis point of view.

Sound examples are available at:
http://www.lma.cnrs-mrs.fr/∼ guillemain/index.html

Acknowledgement

The authors thanks gratefully René Caussé from IRCAM, Paris, for providing the impedance measurement and the profile of the trumpet, and Jean-Pierre Dalmont, from LAUM, Le Mans, for providing the saxophone impedance measurement.

References

[1] N. Amir, G. Rosenhouse, U. Shimony,"A discrete model for tubular acoustic systems with varying cross section - The direct and inverse problems. Parts 1 and 2: Theory and experiment", Acustica, 81(5), 450-474. (1995)

[2] A. H. Benade, E. V. Jansson, "On Plane and Spherical Waves in Horns with Nonuniform Flare. I. Theory of Radiation, Resonance Frequencies, and Mode Conversion", Acustica, 31(2), 80-98, (1974).

[3] A. H. Benade, W. B. Richards "Oboe normal mode adjustment via reed and staple proportioning", J. Acoust. Soc. Am., 73(5), 1794-1803 (1983).

[4] A. H. Benade, S. J. Lutgen, "The saxophone spectrum", J. Acoust. Soc. Am, 83(5), 1900-1907, (1988).

[5] R. Caussé, J. Kergomard, X. Lurton, "Input impedance of brass musical instruments - Comparison between experiment and numerical models", J. Acoust. Soc. Am., 75(1), 241-253 (1984).

[6] A. Chaigne, J. Kergomard, "Acoustique des instruments de musique", Belin Ed. Collection Echelles, (2008).

[7] J.-P. Dalmont, B. Gazengel, J. Gilbert, J. Kergomard, "Some aspects of tuning and clean intonation in woodwinds", Applied Acoustics 46, 19-60 (1995).

[8] B. Gazengel, J. Gilbert, N. Amir, "From the measured input impedance to the synthesis signal : where are the traps ?", Acta Acustica 3, 445-472, (1995).

[9] P. Guillemain, J. Kergomard, T. Voinier, "Real-time synthesis of clarinet-like instruments using digital impedance models", J. Acout. Soc. Am., 118(1), 483-494, (2005).

[10] N. Hansen. "The CMA Evolution Strategy: A Comparing Review". In J.A. Lozano, P. Larranga, I. Inza and E. Bengoetxea (Eds.). Towards a new evolutionary computation. Advances in estimation of distribution algorithms. pp. 75-102, Springer, (2006).

[11] W. Kausel, "Bore reconstruction of tubular ducts from its acoustic input impedance curve", Proceedings of the 20th IEEE, IMTC'03, 993-998, (2003).

[12] J. Kergomard, "Tone hole external interactions in woodwinds musical instruments", Proc. 13th ICA, Yugoslavia, Vol.3, 53-56, (1989).

[13] C. J. Nederveen, "Acoustical Aspects of Woodwind Instruments", Frits Knuf, Amsterdam, The Netherlands, 1969. Revised 1998, Northern Illinois University Press DeKalb.

[14] A. D. Pierce, *Acoustics*, (McGraw-Hill, New York 1981), presently available from Acoust. Soc. Am., New York (1990).

[15] R. W. Pyle, "Effective length of horns", J. Acout. Soc. Am., 57(6), 1309-1317, (1975).

[16] G. Scavone "An acoustic analysis of single-reed woodwind instruments with an emphasis on design and performance issues and digital waveguide modeling techniques", Ph. D Thesis, Stanford University, (1997).

[17] R. T. Schumacher, "Ab initio calculations of the oscillation of a clarinet", Acustica, 48 , 71-85 (1981).

[18] D. Sharp, "Acoustic Pulse Reflectometry for the Measurement of Musical Wind Instruments" Ph. D Thesis, University of Edimburg, (1996).

[19] J. O. Smith III, "Principles of Digital Waveguide Models of Musical Instruments", In M. Kahrs and K. Brandenburg, editors, Applications of DSP to Audio and Acoustics, 417-466. Kluwer Academic Publishers, (1998).

[20] M. van Walstijn, J. O. Smith, III, "Use of Truncated Infinite Impulse Response (TIIR) Filters in Implementing Efficient Digital Waveguide Models of Flared Horns and Piecewise Conical Bores with Unstable One-Pole Filter Elements", Proc. ISMA-98, Leavenworth, 309-314, (1998).

[21] M. van Walstijn, M. Campbell. "Discrete-time modelling of woodwind intrument bores using wave variables", J. Acoust. Soc. Am, 113, 575-585, (2003).

[22] http://www.bionik.tu-berlin.de/user/niko